The Mechanism of Increasing Outflow Facility during Washout in the Bovine Eye

Darryl Overby,[1] Haiyan Gong,[2] Guanting Qiu,[2] Thomas F. Freddo,[2] and Mark Johnson[3]

Purpose. To investigate the relationship between outflow facility and separation between the inner wall of the aqueous plexus and the juxtacanalicular connective tissue (JCT) during washout in the bovine eye.

Methods. Facility was recorded during 3 hours of anterior chamber perfusion at 15 mm Hg in eight pairs of bovine eyes. One eye of each pair was then lowered to 0 mm Hg for 1 hour, whereas the fellow eye was kept at 15 mm Hg. After a brief perfusion at 15 mm Hg, both eyes were perfusion fixed and processed for electron microscopy. Micrographs of the inner wall were analyzed for separation from the JCT. To study the role of cellular adhesion between the inner wall and JCT, 12 additional pairs were perfused with integrin-binding peptide (RGD: Arg-Gly-Asp) or sham control peptide (RGE: Arg-Gly-Glu) at 2 μM to 2 mM, before IOP was reduced.

Results. During the first 3 hours, facility increased in both eyes because of "washout." However, after 1 hour of 0 mm Hg, facility decreased by 13% ($P < 0.006$), whereas facility increased by 20% ($P < 0.001$) in the fellow eyes maintained at 15 mm Hg. Two types of separation were observed between the inner wall and JCT: cell–matrix separation between the endothelial cell and basal lamina and matrix–matrix separation between the basal lamina and JCT. A significant positive correlation ($P = 0.042$) was found between the degree of matrix–matrix separation and the change in outflow facility after 1 hour of 0 mm Hg. Compared with RGE control, RGD had no apparent effect on outflow facility ($P > 0.35$) or on the change in outflow facility after 1 hour at 0 mm Hg ($P > 0.15$).

Conclusions. The increase in outflow facility that occurs during washout in the bovine eye is reversible and correlates with the degree of separation between the basal lamina of the inner wall endothelium and the JCT. Therefore, adhesions tethering the inner wall to the JCT may be important ultrastructural features involved in the regulation of aqueous humor outflow resistance. (*Invest Ophthalmol Vis Sci.* 2002;43:3455–3464)

The mechanism responsible for the generation of aqueous humor outflow resistance remains unknown in both the normal and glaucomatous eye. Currently, lack of a thorough understanding of those features responsible for regulating outflow resistance hinders the development of effective antiglaucoma therapy to normalize trabecular outflow. Although several studies have localized the primary site of outflow resistance to within the region near the juxtacanalicular connective tissue (JCT) and the inner wall endothelium of Schlemm's canal,[1–4] the ultrastructural basis for the generation of aqueous humor outflow resistance remains unclear.[5–7]

One hypothesis to explain aqueous outflow resistance is pore funneling, which is a hydrodynamic coupling between the inner wall endothelium of Schlemm's canal and the JCT.[8] This coupling arises from the proximity of these two tissue layers combined with the condition that aqueous must cross the inner wall through discrete pores. Flow through the JCT is thereby confined to regions near the inner wall pores, forcing a funneling pattern of aqueous streamlines, as illustrated in Figure 1A. The reduction in available area for flow increases the effective outflow resistance. The fundamental difference distinguishing the funneling hypothesis from other hypotheses of aqueous outflow is that the net resistance of the inner wall and JCT considered together is greater than the sum of their resistances considered separately.

Support for the funneling hypothesis comes from a recent tracer study investigating the mechanism of H-7,[9] a compound known to reversibly increase outflow facility in monkey eyes in vivo.[10,11] After infusion of H-7, a change from a punctate to a uniform distribution of tracer particles was observed along the inner wall,[9] as would be predicted by disruption of the funneling streamlines.

During prolonged anterior chamber perfusion of nonhuman eyes, outflow facility has been observed to increase in a process that has been termed "washout."[12] Although washout was originally believed to result from a washing away of extracellular matrix from the outflow pathway,[13–16] biochemical studies have failed to demonstrate a significant loss of hyaluronic acid[17] or sulfated proteoglycan[18] during washout, and currently the mechanism of washout remains unexplained. Washout has been observed as a common response to experimental perfusion of eyes of many nonhuman species,[16,19–23] and therefore understanding the basis for washout may provide insight into a general mechanism of outflow resistance while illuminating functional differences in outflow pathway physiology between humans and other species.

In light of the funneling hypothesis, mechanical connectivity between the inner wall and JCT appears critical for the maintenance of outflow resistance. Our goal in this study was to investigate the role of this mechanical connectivity in the regulation of outflow facility. We hypothesize that washout results from a loss of connectivity between the inner wall and JCT, which leads to an increase in outflow facility through an elimination of the funneling effect, as depicted in Figure 1B. We predict that if IOP were lowered to 0 mm Hg after washout, the inner wall and JCT would return to their neutral, adjacent positions and the attachments between the inner wall and JCT that were lost during the washout process would be reestablished and the increase in outflow facility would be reduced or eliminated.

From the [1]Department of Mechanical Engineering, Massachusetts Institute of Technology, Cambridge, Massachusetts; the [2]Department of Ophthalmology, Boston University School of Medicine, Boston, Massachusetts; and the [3]Department of Biomedical Engineering, Northwestern University, Evanston, Illinois.

Supported by The Whitaker Foundation, the National Eye Institute, Grant EY09699, the Glaucoma Research Foundation and unrestricted departmental grants from Research to Prevent Blindness, Inc., and The Massachusetts Lions Eye Research Fund to Boston University.

Submitted for publication September 26, 2001; revised April 26, 2002; accepted May 31, 2002.

Commercial relationships policy: N.

The publication costs of this article were defrayed in part by page charge payment. This article must therefore be marked "*advertisement*" in accordance with 18 U.S.C. §1734 solely to indicate this fact.

Corresponding author: Mark Johnson, Department of Biomedical Engineering, Northwestern University, 2145 Sheridan Road, TECH E354, Evanston, IL 60208; m-johnson2@northwestern.edu.

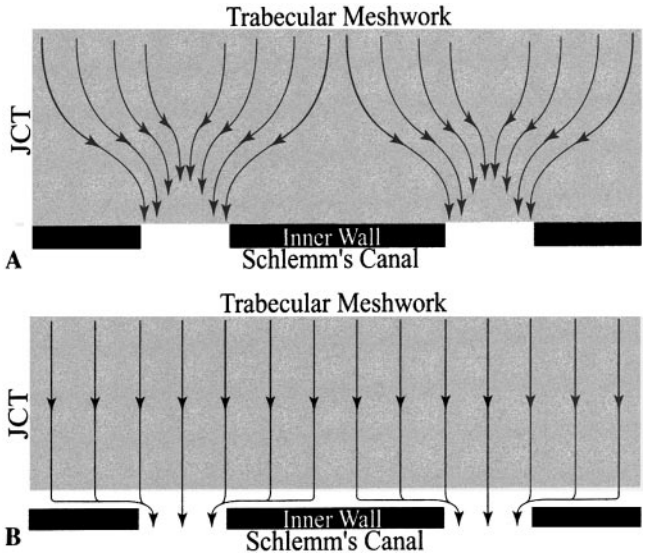

FIGURE 1. An illustration of the streamlines of aqueous flow through the JCT before (**A**) and after (**B**) washout, as predicted by the funneling hypothesis. (**A**) To enter Schlemm's canal, aqueous must converge to pass through discrete openings along the inner wall, which decreases the available area for flow and increases outflow resistance. (**B**) Separation of the inner wall from the JCT eliminates the funneling pattern, increases the available area for flow, and increases outflow facility during washout.

Furthermore, we suspect that some members of the integrin family of transmembrane adhesion proteins, several of which have been identified along the inner wall,[24,25] might be responsible for maintaining the connectivity between the inner wall and JCT. To test this hypothesis, we perfused with soluble peptides containing the integrin-binding amino acid sequence RGD (arginine-glycine-aspartate), and attempted to inhibit the reestablishment of adhesion that we postulated would occur during the period of zero IOP.

MATERIALS AND METHODS

Materials

Twenty pairs of enucleated bovine eyes were obtained from a local abattoir (Arena and Sons, Hopkinton, MA) and delivered on ice within 6 hours after death. Eyes with any discernible damage or accumulated blood in the limbus or anterior chamber were not used. The perfusion fluid was Dulbecco's phosphate-buffered saline (PBS; Life Technologies, Grand Island, NY) containing 5.5 mM D-glucose (collectively referred to as DBG) and was passed through a 0.2-μm cellulose acetate filter before use. The setup of the perfusion system has been described previously.[26,27] Briefly, the perfusion system consists of a computer controlled syringe pump that delivers a variable flow rate, Q, to the anterior chamber so as to maintain a desired IOP that is monitored by a pressure transducer connected electronically to the computer control system (Macintosh G3; Apple Computers, Cupertino, CA). Outflow facility ($C = Q$/IOP) was measured at 10 Hz, ensemble averaged over a 10-second window, and electronically recorded every 10 seconds. Eyes were fixed with freshly made 2.5% glutaraldehyde-2% paraformaldehyde in Sörenson's PBS (pH 7.3). All studies adhered to the ARVO Statement for the Use of Animals in Ophthalmic and Vision Research.

To trace the flow pathway, four pairs of eyes received cationic colloidal gold tracer (5 nm and 10 nm diameter, 10^{12}/mL; Ted Pella, Inc., Redding, CA) dialyzed against PBS. In one pair, a centrifugation method (19,000 revolutions per minute) was used instead and yielded a lower final concentration of colloidal gold (5×10^{10}/mL).

To investigate the role of integrin-based adhesion between the inner wall and JCT, 10 eyes received a solution of glycine-arginine-glycine-aspartate-serine-proline hexapeptide (GRGDSP; Life Technologies) that contained the integrin-binding amino acid sequence RGD.[28] Contralateral eyes received an equivalent concentration of nonbinding glycine-arginine-glycine-glutamate-serine-proline hexapeptide (GRGESP; Life Technologies) as a negative control. Each peptide solution was diluted with DBG to the desired concentration between 2.0 μM and 2.0 mM. To test the potential activity of the flanking peptide sequence, two additional eyes were perfused with glycine-arginine-glycine-aspartate-threonine-proline (GRGDTP; Sigma-Aldrich, St. Louis, MO), and the fellow eyes received the same concentration of GRGDSP. All peptide solutions were refrigerated at 4°C before use and were stored at −20°C.

Perfusion Procedure

Bovine eyes were cleared of extraocular tissue and submerged to the limbus in isotonic saline at 34°C. A 23-gauge infusion needle was inserted intracamerally, with the needle carefully threaded through the pupil and the needle tip positioned within the posterior chamber to prevent deepening of the anterior chamber that would otherwise lead to an artificial increase in outflow facility.[29] Eight pairs of eyes were perfused at 15 mm Hg for 3 hours with DBG, to allow sufficient time for extensive washout while outflow facility was continually recorded. After 3 hours, the perfusion system was paused, and IOP of the experimental eye was reduced to 0 mm Hg by connecting the eye to a reservoir that was slowly lowered to the height of the anterior chamber. To prevent obstruction of the needle by the iris during the period of zero IOP, the needle tip was carefully threaded through the pupil and repositioned within the anterior chamber, taking care to avoid damage to the iris and lens capsule. During this same time, the perfusion in the control eye was continued at 15 mm Hg from a constant-height reservoir with the needle tip remaining in the posterior chamber. Outflow facility was not recorded in either eye during this period.

We hypothesized that during this period of zero pressure, the inner wall and JCT would return to their neutral, adjacent positions and any adhesions between the inner wall and JCT that were disrupted during the washout process would be allowed to re-form. After 1 hour of zero IOP, the needle was threaded through the pupil and returned to the posterior chamber, the perfusion system was restarted at 15 mm Hg in both eyes, and outflow facility was recorded for 30 minutes or until a stable IOP was reached. After this, a second 23-gauge needle was inserted, and the content of the anterior chamber was exchanged with fixative. Perfusion with fixative continued at 15 mm Hg for approximately 30 minutes, to allow adequate fixation of the outflow pathway. Eyes were then sectioned at the equator, placed in fixative overnight at 4°C and transferred to PBS to await further processing.

Four of the aforementioned eight pairs of eyes received cationic colloidal gold tracer to outline the routes of aqueous flow through the JCT. In these eyes, the second intracameral needle was instead inserted into each eye immediately after the period of zero IOP in the experimental eye. DBG containing colloidal gold tracer was then exchanged into the anterior chamber, and both eyes were perfused for 30 minutes at 15 mm Hg or until a stable outflow facility was recorded. In two pairs, fellow eyes received an equivalent volume of tracer solution. After a stable facility value was attained, the anterior chamber was exchanged with fixative, and both eyes were processed as described.

To investigate the role of integrin-based adhesion in the hypothesized reattachment process between the inner wall and JCT, 12 pairs of bovine eyes received various concentrations of RGD peptide before the period of zero IOP. Soluble RGD-containing peptides have been shown to inhibit cellular attachment to several extracellular matrix proteins.[30] Ten pairs of eyes were perfused with DBG at 15 mm Hg for approximately 2.5 hours (range, 1–3.5), followed by insertion of a second intracameral needle and anterior chamber exchange with either GRGDSP or GRGESP peptide solution at 2 μM, 20 μM, 200 μM, or

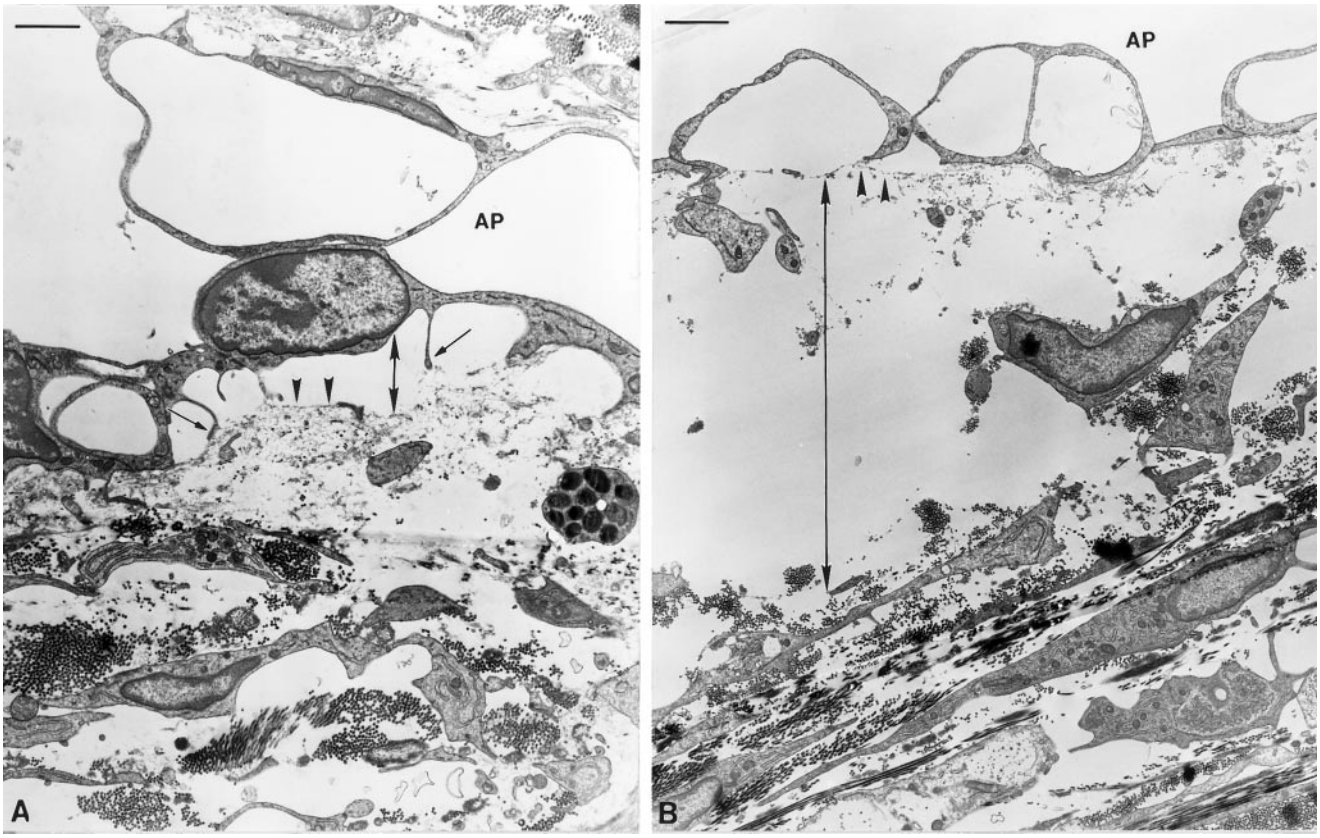

FIGURE 2. (**A**) Cell–matrix separation (*double-headed arrow*) occurred between the endothelial cell and basal lamina (*arrowheads*) along the inner wall of the aqueous plexus (AP). In this image, two inner wall cells were displaced into the lumen, but retained contact with the basal lamina through multiple cellular processes (*arrows*). The extracellular matrix within the JCT remained well organized beneath the site of cell–matrix separation. A giant vacuole was seen extending from the outer wall. (**B**) Matrix–matrix separation (*double-headed arrow*) occurred between the basal lamina (*arrowheads*) of the inner wall and the underlying JCT matrix. The basal lamina remained attached to the inner wall cell, and together they were displaced from the JCT. Bars, 2 μm.

2 mM. After the peptide exchange, perfusion with DBG and peptide continued at 15 mm Hg in both eyes. Approximately 1 hour after the exchange (range, 40–120 minutes), IOP was decreased to 0 mm Hg in both eyes for 1 hour, according to the technique described earlier. After this hour of zero IOP, the perfusion was restarted at 15 mm Hg in both eyes and was continued until a stable facility was recorded. In the remaining two pairs of eyes, specificity to the amino acids flanking the RGD sequence was investigated by exchanging with either 200 μM of GRGDSP or GRGDTP, following the procedure described earlier.

Electron Microscopy

Anterior segments of the eyes were cut into meridional sections (1–2 mm thick) that were postfixed in 2% osmium tetroxide and 1.5% potassium ferrocyanide in buffer for 2 hours. The specimens were then dehydrated in a graded series of ethanol and embedded in Epon-Araldite. Semithin sections for light microscopy were made to identify the outflow region and to localize the inner wall of the aqueous plexus (the bovine equivalent of Schlemm's canal). Ultrathin sections (90 nm) were cut with an ultramicrotome, counterstained with uranyl acetate and lead citrate, and examined by electron microscope (model 300; Phillips, Eindhoven, The Netherlands). Micrographs from two to four different quadrants were taken along the inner wall of the aqueous plexus at an original magnification of 3300×. In those eyes receiving colloidal gold tracer, micrographs were also taken at higher magnification (10,000×), to visualize the distribution of the gold particles.

Grading the Extent of Separation between the Inner Wall and JCT

During the present study, two types of separation were observed between the JCT and the inner wall of the aqueous plexus that could potentially reduce outflow resistance according to the funneling hypothesis: cell–matrix separation between endothelial cells and their basal lamina and matrix–matrix separation between the extracellular matrix of the JCT and the basal lamina of the inner wall. An example of the former is shown in Figure 2A and is characterized by displacement of the cell into the lumen and the formation of giant vacuoles and parachute-like tethers that retained focal contacts with the basal lamina.[31] Matrix–matrix separation, such as that seen in Figure 2B, is characterized by a loss of adhesion and a discernible separation between the basal lamina and the extracellular matrix of the JCT and is usually associated with a loose or "relaxed" JCT matrix.

A trained masked observer (HG) was presented with randomly selected micrographs of the inner wall and JCT from the eight pairs of eyes that did not receive RGD peptide and was instructed to identify regions along the inner wall that exhibited cell–matrix and matrix–matrix separations. As an aide in the identification of each type of separation, the observer was asked to first identify the clearest demarcation of the basal lamina along the inner wall endothelium. From this boundary, cell–matrix separation could be easily evaluated by an absence of endothelial juxtaposition. Matrix–matrix separation may also be judged from an absence or paucity of extracellular material immediately beneath the identified basal lam-

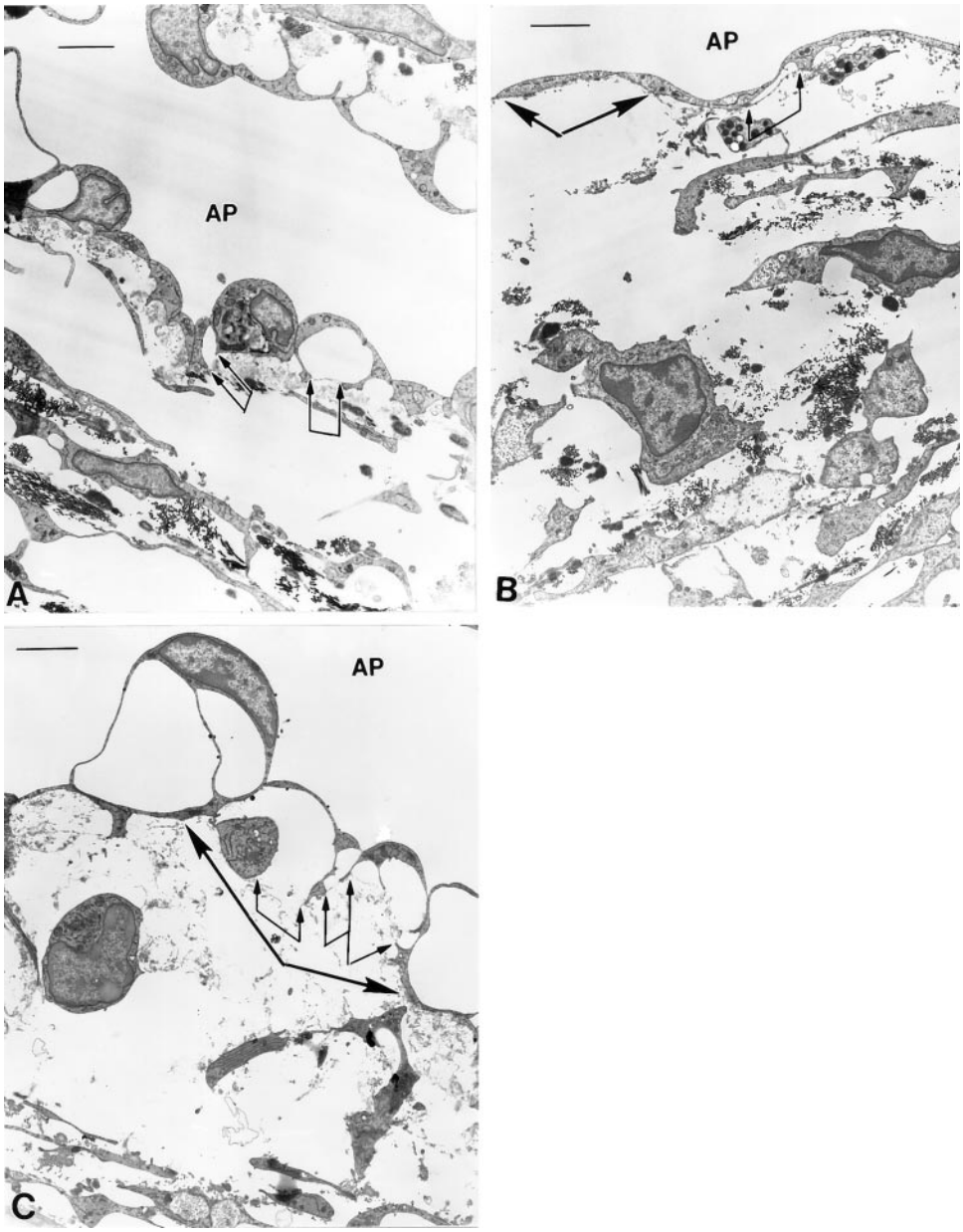

FIGURE 3. Examples of scoring for cell–matrix (between *small arrowheads*) and matrix–matrix separation (between *large arrowheads*). (**A**) Cell–matrix: 1, matrix–matrix: 0; (**B**) cell–matrix: 1, matrix–matrix: 2; (**C**) cell–matrix: 2, matrix–matrix: 2. AP, aqueous plexus. Bars, 2 μm.

ina. Regions defined for each type of separation were allowed to overlap.

Each micrograph received two scores based on qualitative observation of the fraction of inner wall length appearing to exhibit each type of separation. If separation was evident for less than approximately one third of the length of the inner wall shown in the micrograph, a score of 1 was assigned. If separation extended more than approximately one third the length of the inner wall in the micrograph, a score of 2 was assigned. Finally, if more than two thirds the length of the inner wall present in the micrograph was separated, a score of 3 was assigned. If no separation was observed, a score of 0 was assigned. Scores of all micrographs of a given eye were pooled and averaged for each type of separation. At least 10 micrographs from at least two different quadrants were analyzed per eye. All micrographs were printed at the same final magnification and showed nearly equivalent lengths of the inner wall. Examples of scoring for three micrographs are shown in Figure 3.

The variability of assigned scores was examined by having the same masked observer reexamine 50 of the previously scored micrographs 1 month after the first analysis. Between the two trials, cell–matrix and matrix–matrix scores were identical in 72% and 70% of the micrographs, respectively, and of the differences in scores, more than 90% were 1 point on the scoring scale. The remaining differences were 2 points; no scores differed by 3 points.

Statistical Methods

Two-tailed Student's *t*-test and linear regression analysis were applied (Systat for the Macintosh, ver. 5.2.1; SPSS, Chicago, IL) with a required significance level of 0.05. For the regressions, the residuals (the difference between the fitted value of the dependent parameter and its measured value) were examined and in all cases appeared random when plotted against the independent variables. Outliers from the fit and points with high leverage were identified by the following criteria: the externalized studentized residual (analogous to a *t*-statistic) had a probability of occurrence that was less than $0.05/N$ (where N is the number of data points) or the Cook distance was greater than 1.[32] Based on these criteria, no data points were excluded from the statistical analysis described in the Results section.

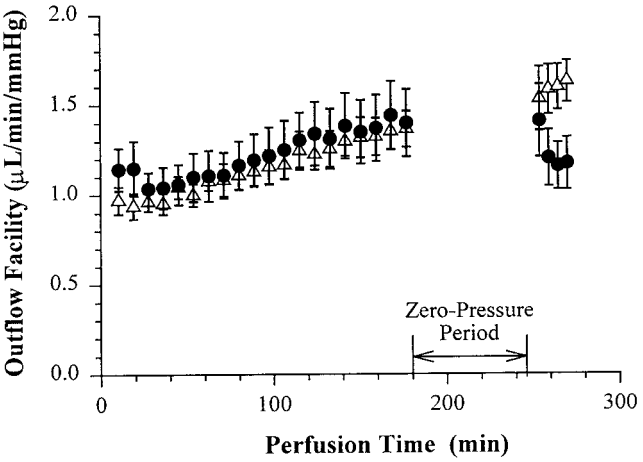

FIGURE 4. Measured outflow facility in four pairs of eyes perfused throughout at 15 mm Hg (△) and perfused at 15 mm Hg with perfusion interrupted by a 1-hour period of 0 mm Hg (●). Error bars, SE.

RESULTS

Results are summarized in this article. A more detailed compilation of results has been published in Overby.[33]

Outflow Facility

Measured outflow facility in four pairs of eyes is shown in Figure 4. (Data from the latter four pairs of eyes are not included in Fig. 4, because the time course of the experiment was different in those eyes receiving colloidal gold.) Outflow facility began with a baseline near 1.0 μL/min · mm Hg, which increased comparably in both eyes because of washout. At 3 hours, the perfusion of the experimental eye was halted, and IOP was decreased to 0 mm Hg for 1 hour, while the perfusion of the control eye was continued at 15 mm Hg. Throughout this period, outflow facility of the control eye increased and seemed to follow the same course of washout. However, the outflow facility of the experimental eye decreased, and a significant fraction of the increase in outflow facility due to washout appears to have been recovered.

A summary of outflow facility data from all eight pairs of eyes is presented in Table 1. Both the mean baseline outflow facility (C_0) and the mean facility after 3 hours of perfusion (C_1) were similar between control and experimental eyes ($P > 0.8$ and $P > 0.6$, respectively). In every experimental eye, the outflow facility C_2 decreased after the period of zero IOP, whereas in every control eye, outflow facility increased during this period. C_2 was determined after a stable facility level was achieved (20–30 minutes after IOP was increased to 15 mm Hg) by averaging over 5 to 10 minutes of consecutive facility data. In the experimental eye, the change in outflow facility after the period of zero pressure ($C_2 - C_1$) decreased by 13% ($P < 0.006$), whereas in the control eye, $C_2 - C_1$ increased by 20% ($P < 0.001$). These results demonstrate that the increase in outflow facility due to washout was partly reversible by reduction of IOP to 0 mm Hg for 1 hour.

Morphologic Evaluation

Significant differences were seen in the morphology of the inner wall and JCT in control eyes after washout compared with experimental eyes after reversal of washout (Fig. 5). In control eyes, the inner wall appeared distended, the JCT appeared loose and disorganized, and frequent herniations of the inner wall and JCT were observed protruding into the lumen of the aqueous plexus. In contrast, the inner wall of experimental eyes appeared more in contact with underlying structures, the JCT appeared more compact, and fewer herniations were observed along the inner wall.

To investigate the relationship between outflow facility and morphology, 235 micrographs of the inner wall and JCT were analyzed and scored, based on the length of inner wall exhibiting cell–matrix and matrix–matrix separation. A summary of the scoring results obtained from a trained masked observer (HG) is shown in Table 2. No statistically significant difference in cell–matrix separation was found between the control and experimental groups ($P > 0.75$). There was a tendency to see a greater matrix–matrix separation in the control than in the experimental group, but this difference was not statistically significant ($P > 0.17$).

The variable of interest in this study was the change in outflow facility $C_2 - C_1$ that occurred after the hour-long period of zero IOP in the experimental eye. There was no correlation between this facility change and the extent of cell–matrix separation ($P > 0.5$). However, as shown in Figure 6, there was a statistically significant correlation between $C_2 - C_1$ and the extent of matrix–matrix separation ($P = 0.042$).

TABLE 1. Outflow Facility for Experimental Eyes Undergoing 1 Hour of 0 mm Hg IOP Versus Control Eyes Maintained at 15 mm Hg

	Outflow Facility*							
	C_0: Baseline		C_1: Pre–Zero IOP		C_2: Post–Zero IOP		C_3: Post-Fixation	
Pair	Exp.	Cont.	Exp.	Cont.	Exp.	Cont.	Exp.	Cont.
1	1.19	1.11	1.46	1.61	1.14	2.00	0.27	0.67
2	0.98	0.95	1.45	1.28	1.27	1.50	0.31	0.49
3	1.28	0.84	1.81	1.14	1.47	1.40	0.55	0.54
4	0.78	0.94	0.90	1.45	0.80	1.65	0.25	0.57
5†	1.58	2.09	2.90	3.69	2.55	4.70‡	1.16‡	2.31‡
6†	1.09	1.14	1.38	1.72	1.06	2.10	0.62	0.93
7†	1.51	1.30	2.24	2.51	2.13	3.35	0.90	1.39
8†	0.83	1.00	1.15	1.28	1.11	1.30	0.29	0.47
Mean ± SE	1.16 ± 0.10	1.17 ± 0.14	1.66 ± 0.23	1.83 ± 0.30	1.44 ± 0.21	2.25 ± 0.42	0.54 ± 0.12	0.92 ± 0.23

Exp., experimental group; Cont., control group.

* Outflow facility ($C = Q/IOP$) is expressed in units of μL/min/mm Hg and was computed by averaging over 5 to 10 consecutive minutes of electronic data.

† These eyes received colloidal gold tracer.

‡ A computer failure occurred during the perfusion of these eyes, and facility was computed from hand-recorded notes.

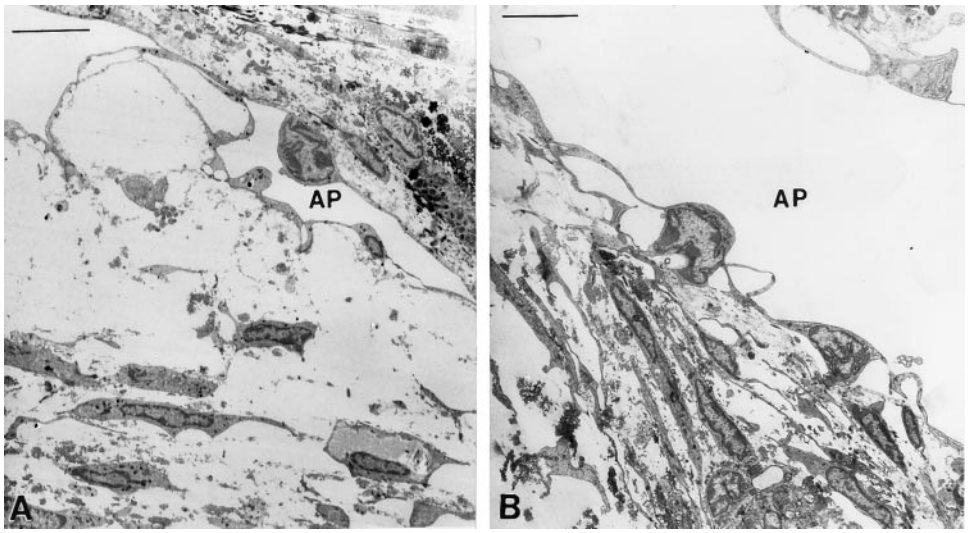

FIGURE 5. Representative electron micrographs from paired eyes showing the morphology of the inner wall of the aqueous plexus (AP) and JCT for the high-facility state after prolonged washout (**A**) compared with the low-facility state after pressure-induced reversal of washout (**B**). The morphology shown in (**A**) exhibits both cell–matrix and matrix–matrix separation. Bars, 5 μm.

In the bovine eye, variability in the size of outflow pathway tissues has been observed around the circumference of the iris.[34] The possibility that this variability may attribute to differences in cell–matrix or matrix–matrix separation was examined by comparing morphologic scores for each eye with the anterior–posterior extent of the outflow region (i.e., the distance between the scleral spur and the Schwalbe line), and with the length of plexus inner wall contacting the trabecular meshwork. Each of these quantities was measured from corresponding light micrographs from the same quadrant and was analyzed using linear regression. No statistical relationship was observed between either the assigned cell–matrix or matrix–matrix scores and the anterior–posterior extent of the outflow region ($P > 0.90$ and $P = 0.60$, respectively; $n = 16$) or between the assigned scores and length of plexus inner wall ($P > 0.12$ and $P > 0.90$ for cell–matrix and matrix–matrix scores, respectively; $n = 16$).

Distribution of Colloidal Gold Tracer

Using electron microscopy, colloidal gold was found to be associated with extracellular matrix underneath the inner wall endothelium in control eyes (Fig. 7A). Consistently fewer particles were found within the JCT of experimental eyes, despite the nearly equivalent volume of colloidal gold perfused through each eye of a pair. Gold was especially sparse in the more compact regions of the JCT in experimental eyes (Fig. 7B). Difficulty in locating colloidal gold along the inner wall and within the JCT of experimental eyes prevented a more thorough investigation of the tracer distribution.

Influence of Soluble RGD on Reversal of Washout

The presence of RGD-dependent integrins has been identified within the region of the JCT and inner wall of Schlemm's canal,[24,25] and we postulated that these integrin connections might be active in the reattachment process hypothesized to occur during reversal of washout. To explore this possibility, we perfused soluble RGD peptide at various concentrations before reducing IOP in an attempt to inhibit the pressure-induced reversal of washout and perfused contralateral eyes with RGE peptide as a control. To investigate whether the extraneous peptide sequence had an effect on the hypothesized integrin adhesion, we also perfused two eyes with 200 μM GRGDTP, whereas the contralateral eyes received the same concentration of GRGDSP.

Outflow facility from a pair of eyes perfused at 15 mm Hg, and exchanged with either 2 mM GRGDSP or GRGESP peptide, is shown in Figure 8. After the hour-long period of zero IOP in both eyes, outflow facility decreased, despite perfusion with a large concentration of RGD peptide. After the reversal of washout, outflow facility increased once again in both eyes at a rate similar to the rate observed before the peptide exchange.

A summary of the remaining 11 pairs of eyes receiving RGD peptide is presented in Table 3. The decrease in outflow facility after zero IOP persisted at all concentrations of RGD investi-

TABLE 2. Average Scores for Cell–Matrix and Matrix–Matrix Separation for Experimental Eyes Undergoing 1 Hour of 0 mm Hg IOP Versus Control Eyes Maintained at 15 mm Hg

	Quadrants (n)		Micrographs (n)		Score for Cell–Matrix Separation		Score for Matrix–Matrix Separation	
Pair	Exp.	Cont.	Exp.	Cont.	Exp.	Cont.	Exp.	Cont.
1	2	2	12	10	1.33 ± 0.19	1.40 ± 0.16	0.33 ± 0.14	1.60 ± 0.40
2	3	2	12	19	1.42 ± 0.19	1.42 ± 0.16	0.92 ± 0.29	0.58 ± 0.19
3	2	2	21	13	1.43 ± 0.13	1.31 ± 0.13	1.19 ± 0.27	0.46 ± 0.22
4	3	2	12	12	1.08 ± 0.08	1.25 ± 0.13	0.75 ± 0.28	0.92 ± 0.36
5	3	3	12	17	1.00 ± 0.12	1.35 ± 0.19	1.08 ± 0.23	1.82 ± 0.31
6	2	4	12	18	1.42 ± 0.19	1.33 ± 0.11	0.08 ± 0.08	0.33 ± 0.11
7	3	2	18	17	1.61 ± 0.16	1.41 ± 0.15	0.61 ± 0.26	1.47 ± 0.30
8	3	2	18	12	1.39 ± 0.18	1.00 ± 0.17	0.94 ± 0.22	1.50 ± 0.34
Mean ± S.E.					1.33 ± 0.07	1.31 ± 0.05	0.74 ± 0.13	1.09 ± 0.21

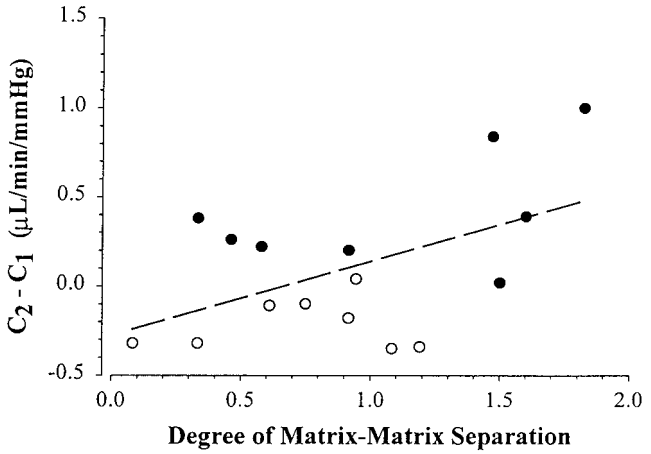

FIGURE 6. The change in outflow facility ($C_2 - C_1$) as a function of assigned matrix–matrix score. (○) Experimental eyes (pressure lowered from 15 mm Hg to 0 mm Hg between C_1 and C_2). (●) Control eyes (pressure maintained throughout at 15 mm Hg). *Dashed line*: best linear fit to all the data ($P = 0.042$). C_1, average facility measured over 5 to 10 minutes immediately before 0 mm Hg IOP; C_2, average facility measured over 5 to 10 minutes after 0 mm Hg IOP, immediately before fixative exchange.

gated, and no significant difference in the decrease in outflow facility after zero IOP was observed between those eyes receiving RGD and control eyes receiving RGE ($P > 0.15$, at all concentrations). At each peptide concentration investigated, the average decrease in outflow facility after zero IOP was no less than the 13% decrease observed in the absence of peptide (Table 1). Furthermore, no significant difference was observed in the decrease in outflow facility after zero IOP between those eyes receiving 200 µM GRGDTP and the contralateral eyes receiving the same concentration of GRGDSP ($P > 0.3$). After exchange with RGD peptide, an increase in facility was observed in some eyes, but this increase was not statistically significant when compared as a group with control eyes receiving RGE peptide ($P > 0.35$, at all concentrations).

DISCUSSION

In this study, we investigated the mechanism underlying the increase in outflow facility that characterizes the washout effect in the bovine eye, hoping to better understand the morphologic features that govern aqueous outflow resistance in general. In our results, (1) much of the increase in outflow facility during washout was rapidly reversed by reducing IOP to 0 mm Hg, (2) the degree of washout reversal correlated with

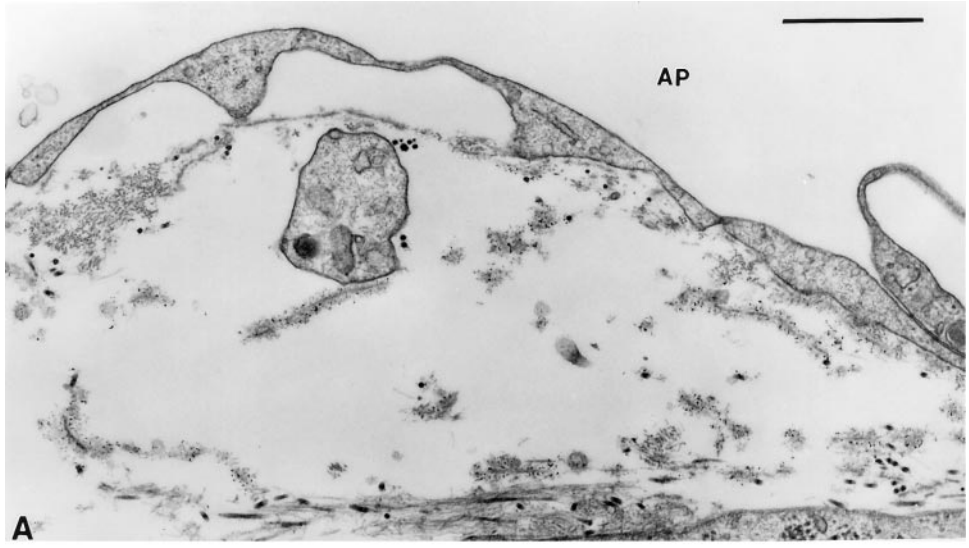

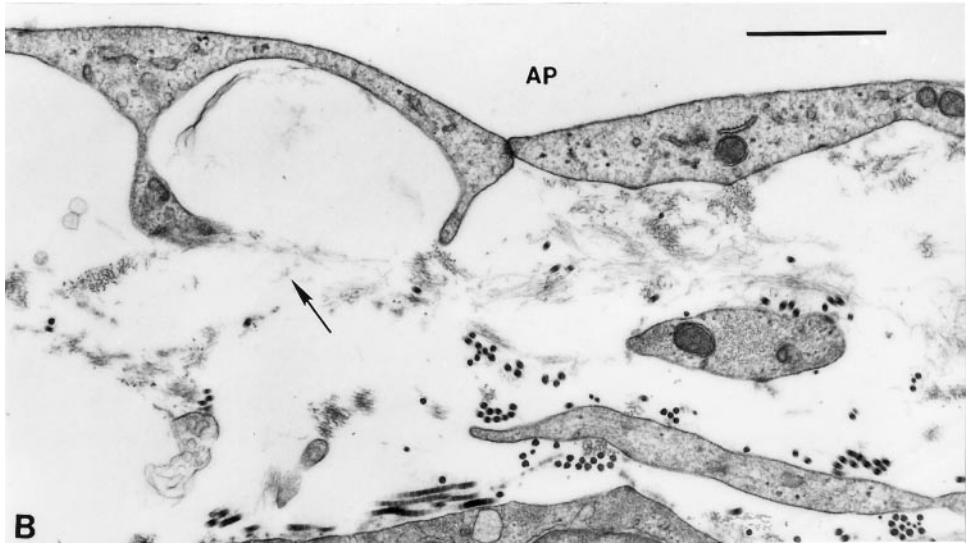

FIGURE 7. Distribution of cationic colloidal gold particles (5 and 10 nm) within the JCT and along the inner wall of the aqueous plexus (AP) in a control eye after extended washout (**A**) and in the fellow experimental eye after pressure-induced reversal of washout (**B**). In the control eye, numerous particles were usually found associated with extracellular matrix beneath the inner wall (fine *black* particles). In the experimental eye, gold particles were rarely observed along the inner wall and in the JCT (**B**, *arrow*). Both eyes received an equivalent volume of colloidal gold tracer. Bars, 1 µm.

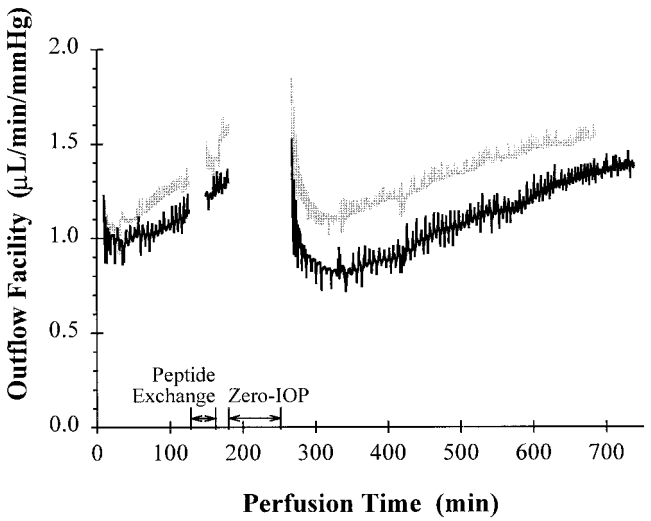

FIGURE 8. Measured outflow facility in a pair of eyes perfused at 15 mm Hg and receiving 2.0 mM of either GRGDSP (*gray trace*) or GRGESP (*black trace*) peptide followed by a 1-hour period at 0 mm Hg IOP in both eyes. Outflow facility was observed to decrease in both eyes after the period of zero IOP. However, facility increased again after reversal of washout.

a decrease in apparent separation between the JCT and the basal lamina of the inner wall, and (3) pressure-induced reversal of washout occurred regardless of the presence of soluble RGD peptide. These results imply that washout acts through a reversible mechanism that is associated with separation of the basal lamina of the inner wall from the underlying JCT. Most important, these results suggest that aqueous outflow resistance in vivo may be regulated by the degree of mechanical connectivity between the inner wall and JCT.

Washout was first recognized by Bárány and Scotchbrook,[13] who attributed the increase in outflow facility to a "washing away" of extracellular material—namely, hyaluronate—thought to be responsible for generating outflow resistance.[13,14,16] However, the reversible nature of washout has not been reported, and our observation that washout may be reversed within an hour seems inconsistent with the time necessary for secretion and organization of significant quantities of extracellular matrix.[35] This finding, combined with the findings of Knepper et al.[17] and Johnson et al.[18] that neither hyaluronate nor sulfated proteoglycans are depleted from the outflow pathway during washout, further challenges the argument that washout results from a loss of extracellular matrix from the outflow pathway during perfusion.

Previous investigators have reported similar matrix–matrix and cell–matrix separations in response to elevated intraocular pressure.[36–38] "Ballooning" of the inner wall, morphologically similar to matrix–matrix separation, has been observed at physiologic pressures in the pig[39] and in primates after extended perfusion.[40] Facility-increasing drugs, such as H-7[9] and Y-27632,[41] have also been shown to induce a marked expansion of the JCT and distention of the inner wall.

In the present study, we identified a correlation between the decrease in outflow facility after reversal of washout and a reduction in the separation between the JCT and the basal lamina of the inner wall. This suggests that washout proceeds through a loss of connectivity between the JCT and inner wall. Although we suspected outflow resistance to decrease through an elimination of the funneling effect, difficulty in locating colloidal gold along the inner wall and JCT within the experimental eyes prevented an adequate investigation of this hypothesis. The relative absence of colloidal gold from the JCT region of the experimental eyes was surprising, particularly because control and experimental eyes were perfused with nearly equivalent volumes of tracer solution. Nevertheless, these results were consistent with a previous report that also found an absence of tracer material immediately underneath the inner wall of Schlemm's canal after perfusion, despite its presence within the canal lumen.[42] It is not clear whether our results were due to altered binding characteristics, altered flow patterns, or another phenomenon.

Circumferential variability in the anterior–posterior extent of the aqueous outflow pathway has been noted in the bovine eye,[34] and we therefore examined the possibility that such variability could be responsible for the observed relationship between the assigned matrix–matrix score and outflow facility (Fig. 6). However, we were unable to find any significant correlation between the assigned scores for cell–matrix and matrix–matrix separation and either the anterior–posterior extent of the outflow pathway or the length of plexus inner wall contacting the trabecular meshwork. Although these findings do not completely rule out all influence of circumferential variability, they do suggest that circumferential variability is not the primary factor contributing to the statistically significant relationship observed between outflow facility and the assigned score for matrix–matrix separation. Furthermore, being that two or more randomly selected quadrants contribute to the average scores for each eye, it seems unlikely that the results shown in Figure 6 arose from circumferential variability between control and experimental eyes.

TABLE 3. Summary of Outflow Facility Data after Exchange with RGD or RGE Peptide Followed by 1 Hour of 0 mm Hg IOP in Both Eyes

Concentration (μM)	*n*	Peptide	Outflow Facility* Baseline (μL/min/mm Hg)	Post/Pre–Peptide Exchange	Post/Pre–Zero IOP
2	3	GRGDSP	0.98 ± 0.10	1.06 ± 0.04	0.73 ± 0.12
		GRGESP	1.06 ± 0.19	1.12 ± 0.03	0.64 ± 0.11
20	4	GRGDSP	1.06 ± 0.04	1.25 ± 0.10	0.67 ± 0.04
		GRGESP	0.99 ± 0.07	1.15 ± 0.03	0.76 ± 0.03
200†	4	GRGDSP	0.88 ± 0.09	1.21 ± 0.04	0.71 ± 0.09
	(2)	GRGDTP	0.82 ± 0.08	1.24 ± 0.04	0.77 ± 0.11
	(2)	GRGESP	1.19 ± 0.22	1.28 ± 0.13	0.75 ± 0.13

* Outflow facility ($C = Q/\text{IOP}$) is expressed in units of μL/min/mm Hg and was computed by averaging over 10 consecutive minutes of electronic data.

† Of the four perfusions, two investigated the difference between GRGDSP and GRGESP and two investigated the difference between GRGDSP and GRGDTP, as indicated by the values given in parentheses.

Integrins are a family of transmembrane receptors responsible for cellular adhesion to a variety of extracellular proteins,[28] and the presence of RGD-binding integrins has been identified immunohistochemically within the JCT and along the inner wall endothelium of Schlemm's canal.[24,25] We suspected that integrins are normally involved in mechanically tethering the inner wall to the JCT, and we hypothesized that re-formation of integrin adhesions may be responsible for the return of outflow resistance during the period of zero IOP. However, attempts to inhibit this hypothesized reattachment process with soluble RGD peptide had no effect on reversal of washout at any peptide concentration (2 μM to 2 mM) investigated in this study. These results imply that the restoration of outflow facility during the period of zero IOP is not mediated through a reestablishment of RGD-dependent integrins. These implications are consistent with the finding that washout is associated with a separation between the matrix of the JCT and basal lamina rather than between the basal lamina and endothelial cell, which is the more likely site of integrin-based adhesion. Furthermore, perfusion with RGD peptide was not observed to significantly increase outflow facility compared with control eyes receiving RGE, contrary to reports from recent studies in porcine eyes.[43] These discrepant results could indicate species-dependent differences in the role of integrin-based adhesion toward the generation of outflow resistance.

In light of the current results, washout in the bovine eye seems to function as a mechanism to regulate IOP. Elevation in IOP increases the pressure difference across the outflow pathway (i.e., IOP minus episcleral venous pressure) that is known to distend the inner wall and underlying tissues,[36,37] straining the connecting fibrils tethering the inner wall to the JCT and driving their eventual separation. This pressure-induced separation then acts to increase outflow facility and oppose the increase in IOP. In the present study, this pressure difference was larger than it would be physiologically, because the episcleral venous pressure in enucleated eyes is zero.

The results of this study strongly suggest that the connecting fibrils and molecular constituents responsible for tethering the inner wall basal lamina to the JCT are important regulators of aqueous outflow resistance. In the human eye more than in eyes of any other species, an elastic-like cribriform network extends from the tendons of the ciliary muscle to form extensive connections with the inner wall endothelium.[44] This network may be structurally important for maintaining connectivity between the inner wall and JCT and thus contribute to the regulation of outflow resistance and may be responsible for the apparent absence of washout in the human eye.[12] Indeed, an understanding of why washout has not been observed in the human eye may provide valuable insight into why the human eye is vulnerable to primary open-angle glaucoma.

In summary, we investigated the mechanism for the increase in outflow facility during washout in the bovine eye. In our experiments, washout occurred through a reversible process that was associated with separation of the basal lamina of the inner wall endothelium from the underlying JCT. Because the efficacy of facility-increasing drugs is often evaluated in animal studies, in which washout probably influences measurements of outflow facility, a better understanding of the mechanism responsible for washout is likely to aid in the interpretation of these pharmacologic results. Finally, this study suggests that the adhesive elements between the inner wall and JCT are important regulators of aqueous outflow resistance and therefore represent targets for future research directed against the elevated outflow resistance encountered during glaucoma.

Acknowledgments

The authors thank Rozanne Richman, MS, for technical assistance.

References

1. Grant WM. Further studies on facility of flow through the trabecular meshwork. *Arch Ophthalmol.* 1958;60:523–533.
2. Grant WM. Experimental aqueous perfusion in enucleated human eyes. *Arch Ophthalmol.* 1963;69:783–801.
3. Mäepea O, Bill A. The pressures in the episcleral veins, Schlemm's canal and the trabecular meshwork in monkeys: effects of changes in intraocular pressure. *Exp Eye Res.* 1989;49:645–663.
4. Mäepea O, Bill A. Pressures in the juxtacanalicular tissue and Schlemm's canal in monkeys. *Exp Eye Res.* 1992;54:879–883.
5. Bill A, Svedbergh B. Scanning electron microscopic studies of the trabecular meshwork and the canal of Schlemm: an attempt to localize the main resistance to outflow of aqueous humor in man. *Acta Ophthalmol.* 1972;50:295–320.
6. Johnson M, Kamm RD. The role of Schlemm's canal in aqueous outflow from the human eye. *Invest Ophthalmol Vis Sci.* 1983;24:320–325.
7. Ethier CR, Kamm RD, Palaszewski BA, Johnson M, Richardson TM. Calculations of flow resistance in the juxtacanalicular meshwork. *Invest Ophthalmol Vis Sci.* 1986;27:1741–1750.
8. Johnson M, Shapiro A, Ethier CR, Kamm RD. Modulation of outflow resistance by the pores of the inner wall endothelium. *Invest Ophthalmol Vis Sci.* 1992;33:1670–1675.
9. Sabanay I, Gabelt BT, Tian B, Kaufman PL, Geiger B. H-7 effects on the structure and fluid conductance of monkey trabecular meshwork. *Arch Ophthalmol.* 2000;118:955–962.
10. Tian B, Kaufman P, Volberg T, Gabelt B, Geiger B. H-7 disrupts the actin cytoskeleton and increases outflow facility. *Arch Ophthalmol.* 1998;116:633–643.
11. Tian B, Gabelt B, Peterson J, Kiland J, Kaufman P. H-7 increases trabecular facility and facility after ciliary muscle disinsertion in monkeys. *Invest Ophthalmol Vis Sci.* 1999;40:239–242.
12. Erickson-Lamy K, Schroeder AM, Bassett-Chu S, Epstein DL. Absence of time-dependent facility increase ("washout") in the perfused enucleated human eye. *Invest Ophthalmol Vis Sci.* 1990;31:2384–2388.
13. Bárány EH, Scotchbrook S. Influence of testicular hyaluronidase on the resistance to flow through the angle of the anterior chamber. *Acta Physiol Scand.* 1954;30:240–248.
14. Bárány EH, Woodin AM. Hyaluronic acid and hyaluronidase in the aqueous humor and the angle of the anterior chamber. *Acta Physiol Scand.* 1955;33:257–290.
15. Melton CE, DeVille WB. Perfusion studies on eyes of four species. *Am J Ophthalmol.* 1960;50:302–308.
16. Van Buskirk MS, Brett J. The canine eye: in vitro dissolution of the barriers to aqueous outflow. *Invest Ophthalmol Vis Sci.* 1978;17:258–263.
17. Knepper PA, Farbman AI, Telser AG. Exogenous hyaluronidases and degradation of hyaluronic acid in the rabbit eye. *Invest Ophthalmol Vis Sci.* 1984;25:286–293.
18. Johnson M, Gong H, Freddo TF, Ritter N, Kamm R. Serum proteins and aqueous outflow resistance in bovine eyes. *Invest Ophthalmol Vis Sci.* 1993;34:3549–3557.
19. Bárány EH. Simultaneous measurement of changing intraocular pressure and outflow facility in the vervet monkey by constant pressure infusion. *Invest Ophthalmol.* 1964;3:135–143.
20. Kaufman PL, True-Gabelt B, Erickson-Lamy KA. Time-dependence of perfusion outflow facility in the cynomolgus monkey. *Curr Eye Res.* 1988;7:721–726.
21. Gaasterland DE, Pederson JE, MacLellan HM. Perfusate effects upon resistance to aqueous humor outflow in the rhesus monkey eye. *Invest Ophthalmol Vis Sci.* 1978;17:391–397.
22. Yan DB, Trope GE, Ethier CR, Menon IA, Wakeham A. Effects of hydrogen peroxide-induced oxidative damage on outflow facility and washout in pig eyes. *Invest Ophthalmol Vis Sci.* 1991;32:2515–2520.

23. Bárány EH. In vitro studies of the resistance to flow through the angle of the anterior chamber. *Acta Soc Med Uppsala.* 1953;59: 260–276.
24. Tervo K, Päällysaho T, Virtanen I, Tervo T. Integrins in human anterior chamber angle. *Graefes Arch Clin Exp Ophthalmol.* 1995; 233:291–292.
25. Zhou L, Maruyama I, Li Y, Cheng E, Yue B. Expression of integrin receptors in the human trabecular meshwork. *Curr Eye Res.* 1999; 19:395–402.
26. Sit AJ, Coloma FM, Ethier CR, Johnson M. Factors affecting the pores of the inner wall endothelium of Schlemm's canal. *Invest Ophthalmol Vis Sci.* 1997;38:1517–1525.
27. Sit AJ, Gong H, Ritter N, Freddo TF, Kamm RD, Johnson M. The role of soluble proteins in generating aqueous outflow resistance in the bovine and human eye. *Exp Eye Res.* 1997;64:813–821.
28. Hynes R. Integrins: versatility, modulation, and signaling in cell adhesion. *Cell.* 1992;69:11–25.
29. Ellingsen B, Grant W. Influence of intraocular pressure and trabeculotomy on aqueous outflow in enucleated monkey eyes. *Invest Ophthalmol Vis Sci.* 1971;10:705–709.
30. Hayman E, Pierschbacher M, Ruoslahti E. Detachment of cells from culture substrate by soluble fibronectin peptides. *J Cell Biol.* 1985; 100:1948–1954.
31. Johnstone MA. Pressure-dependent changes in nuclei and the process origins of the endothelial cells lining Schlemm's canal. *Invest Ophthalmol Vis Sci.* 1979;18:44–51.
32. Weisberg S. *Applied Linear Regression.* New York: John Wiley & Sons; 1985:114–121.
33. Overby D. The hydrodynamics of aqueous outflow. In: *Mechanical Engineering.* Cambridge, MA: Massachusetts Institute of Technology; 2002. Thesis.
34. Flügel C, Tamm E, Lütjen-Drecoll E. Different cell populations in bovine trabecular meshwork: an ultrastructural and immunocytochemical study. *Exp Eye Res.* 1991;52:681–690.
35. Hascall V, Heinegård D, Wight T. Proteoglycans: metabolism and pathology. In: Hay ED, ed. *Cell Biology of Extracellular Matrix.* New York: Plenum Press; 1991;149–175.
36. Johnstone MA, Grant WM. Pressure dependent changes in the structures of the aqueous outflow system of human and monkey eyes. *Am J Ophthalmol.* 1973;75:365–383.
37. Grierson I, Lee W. Changes in the monkey outflow apparatus at graded levels of intraocular pressure: a qualitative analysis by light microscopy and scanning electron microscopy. *Exp Eye Res.* 1974; 19:21–33.
38. Grierson I, Lee WR. The fine structure of trabecular meshwork at graded levels of intraocular pressure. *Exp Eye Res.* 1975;20:505–521.
39. McMenamin PG, Steptoe RJ. Normal anatomy of the aqueous humour outflow system in the domestic pig eye. *J Anat.* 1991;178: 65–77.
40. McMenamin PG, Lee WR. Effects of prolonged intracameral perfusion with mock aqueous humour on the morphology of the primate outflow apparatus. *Exp Eye Res.* 1986;43:129–141.
41. Rao PV, Deng PF, Kumar J, Epstein DL. Modulation of aqueous humor outflow facility by the Rho kinase-specific inhibitor Y-27632. *Invest Ophthalmol Vis Sci.* 2001;42:1029–1037.
42. MacRae D, Sears ML. Peroxidase passage through the outflow channels of human and rhesus eyes. *Exp Eye Res.* 1970;10: 15–18.
43. Kumar J, Rao PV, Epstein DL. Modulation of aqueous outflow facility by an integrin-ECM directed RGD peptide [ARVO Abstract]. *Invest Ophthalmol Vis Sci.* 2000;41:**S**754. Abstract nr 4005.
44. Rohen JW, Futa R, Lütjen-Drecoll E. The fine structure of the cribriform meshwork in normal and glaucomatous eye as seen in tangential sections. *Invest Ophthalmol Vis Sci.* 1981;21: 574–585.